Biomed Microdevices (2012) 14:461–469
DOI 10.1007/s10544-011-9623-6

A three-dimensional microfluidic approach to scaling up microencapsulation of cells

Sameer Tendulkar · Sayed-Hadi Mirmalek-Sani · Charles Childers · Justin Saul · Emmanuel C. Opara · Melur K. Ramasubramanian

Published online: 14 January 2012

Abstract Current applications of the microencapsulation technique include the use of encapsulated islet cells to treat Type 1 diabetes, and encapsulated hepatocytes for providing temporary but adequate metabolic support to allow spontaneous liver regeneration, or as a bridge to liver transplantation for patients with chronic liver disease. Also, microcapsules can be used for controlled delivery of therapeutic drugs. The two most widely used devices for microencapsulation are the air-syringe pump droplet generator and the electrostatic bead generator, each of which is fitted with a single needle through which droplets of cells suspended in alginate solution are produced and cross-linked into microbeads. A major drawback in the design of these instruments is that they are incapable of producing sufficient numbers of microcapsules in a short-time period to permit mass production of encapsulated and viable cells for transplantation in large animals and humans. We present in this paper a microfluidic approach to scaling up cell and protein encapsulations. The microfluidic chip consists of a 3D air supply and multi-nozzle outlet for microcapsule generation. It has one alginate inlet and one compressed air intlet. The outlet has 8 nozzles, each having 380 micrometers inner diameter, which produce hydrogel microspheres ranging from 500 to 700 μm in diameter. These nozzles are concentrically surrounded by air nozzles with 2 mm inner diameter. There are two tubes connected at the top to allow the air to escape as the alginate solution fills up the chamber. A variable flow pump 115 V is used to pump alginate solution and Tygon® tubing is used to connect in-house air supply to the air channel and peristaltic/syringe pump to the alginate chamber. A pressure regulator is used to control the flow rate of air. We have encapsulated islets and proteins with this high throughput device, which is expected to improve product quality control in microencapsulation of cells, and hence the outcome of their transplantation.

Keywords Alginate · Microcapsules · Cells · Immunoisolation · Transplantation · Protein · Drug delivery · 3-d microfluidics

S. Tendulkar · M. K. Ramasubramanian
Department of Mechanical & Aerospace Engineering,
North Carolina State University,
Raleigh, NC, USA

M. K. Ramasubramanian
Biomedical Engineering, North Carolina State University,
Raleigh, NC, USA

S.-H. Mirmalek-Sani · C. Childers · J. Saul · E. C. Opara
Institute for Regenerative Medicine,
Wake Forest University Health Sciences,
Winston-Salem, NC, USA

J. Saul · E. C. Opara
School of Biomedical Engineering & Sciences,
Wake Forest University Health Sciences,
Winston-Salem, NC, USA

M. K. Ramasubramanian (✉)
Department of Mechanical & Aerospace Engineering,
North Carolina State University,
Engineering Bldg III, Campus Box 7910, 911 Oval Drive,
Raleigh, NC 27695-7910, USA
e-mail: rammk@ncsu.edu

1 Introduction

Microencapsulation of various materials into spherical hydrogel microcapsules of alginate has found applications in drug delivery, biosensors, microelectronics, bioanalyses, coded imaging aids, cell delivery and cell transplantation due to its biocompatibility and physical properties (Whitesides 2006; Beebe et al. 2002; de Jong et al. 2006). It is emerging

as an efficient technology in the treatment of diabetes, hormone and protein deficient diseases. Some of the major applications include the use of alginate encapsulated islet cells as a form of bioartificial pancreas to treat individuals afflicted with Type 1 diabetes Opara and Kendall (2002); development of a reliable bioartificial liver in the form of encapsulated hepatocytes, for providing temporary but adequate metabolic support to allow spontaneous liver regeneration, or as a bridge to orthotopic liver transplantation for patients with fulminant hepatic failure Joly et al.(1997); use of microcapsules in controlled drug delivery for both clinical and experimental therapeutics (Gombotz and Wee 1998; Moya et al. 2009; Moya et al. 2010). The idea of using microcapsules in the form of spherical hydrogel microcapsules for immune protection of transplanted cells has been around since 1950's. However the inability to produce large scale highly monodisperse microspheres has been a hindrance to this technology. Recent developments in the field of microfluidic systems, biomaterials and manufacturing techniques like lab on chip, photolithography, stereolithography, etc. has given rise to wide variety of research in this field (Li 1998; Orive et al. 2004; Uludag et al. 2000).

A major drawback of the current technologies in use for microencapsulation, namely, the air-syringe pump droplet generator Wolters et al. (1992) and the electrostatic generator Hsu et al. (1994), is that they are incapable of producing sufficient numbers of microcapsules in a short-time period to permit mass production of encapsulated and viable cells for transplantation in large animals and humans De Vos et al. (1997),. It is noteworthy, that a prolonged process of encapsulation adversely affects the viability of the cells. For instance, for transplantation in human subjects, it has been estimated that for the 1 million islets needed for transplantation in a diabetic human subject, about 100 h would be required to complete the encapsulation of this number of islets, assuming one islet/microcapsule. In practice, it has actually been estimated that the duration of the process would be closer to 200 h because of the additional steps involved in the encapsulation procedure, such as permselective coatings and washings, following the generation of the initial cell containing alginate microspheres De Vos et al. (1997). Another drawback of the current microfluidic technologies (Chabert and Viovy 2008) which use oil for shearing of alginate to form monodisperse microcapsules is that it leaves an adhesive oil layer on the surface of the prepared microcapsules which affects the further coating process for preparation of APA microcapsules (Suguira et al. 2007).

Very few technologies like static micro mixers (Haverkamp et al. 1999; Mae et al. 2004), silicon membrane with 200,000 micro fabricated pores (Kobayashi et al. 2005), microfluidic large scale integration chips (Nisisako and Torii 2008) have been able to match the fabrication robustness and production rates that are required for mass manufacturing industrial application. These technologies however face other issues like maintaining the quality of microcapsules produced resulting in slightly polydisperse capsules and complexities with their fabrication and assembly techniques. Also the application of monodispersed hydrogel microcapsules provides distinctive advantages compared to polydispersed ones with respect to detecting, monitoring, predicting, and modeling of their behavior. This situation raises an urgent need for a radically different approach to producing viable encapsulated cells in sufficient quantities rapidly for routine application in human cell therapy.

Fabrication of microfluidic devices has been previously accomplished with the use of various manufacturing techniques like the use of Rapid prototyping technology along with PDMS, softlithography and PDMS, micromachining, micromolding, etc. (Duffy et al. 1998; Narasimhan and Papautsky 2004; Steigert et al. 2007; Beebe et al. 2002). Use of air as a shearing fluid to prepare alginate microcapsules has been implemented using a micro-airflow-nozzle (MAN) by having an alginate channel and air channels next to each other. However MAN is fabricated as different parts which are then assembled and aligned using rubber spacers. This process of alignment and sealing is not simple and can result in leakages during the actual working of the device which gives rise to polydispersity in the output of the device (Suguira et al. 2007). By using rapid prototyping technique for fabrication of our microfluidic device, we have been able to fabricate the entire 3D device as a single part. Our monolithic device removes any requirement for alignment and sealing thus protecting the system for any leakage issues. In this paper, we describe a novel microfluidic approach for producing large numbers of alginate microspheres to encapsulate cells and proteins. We present this new approach and reduce it to practice, by designing and building a prototype, and characterizing the manufacturing process for mass production of alginate microspheres. In addition, we present a 3D microfluidic device which has been fabricated monolithically using Rapid Prototyping technique and finally discuss the results of viability tests that have been performed on the islets encapsulated with our microfluidic device.

2 Materials and methods

2.1 Prototype design and microencapsulation setup

The schematic diagram of the device is shown in Fig. 1. The microfluidic chip capable of producing highly monodisperse droplets consists of a 3D air supply and multi-nozzle outlet for microcapsule generation. It has one alginate inlet and compressed air inlet (Fig. 1(a)). The outlet has 8 nozzles

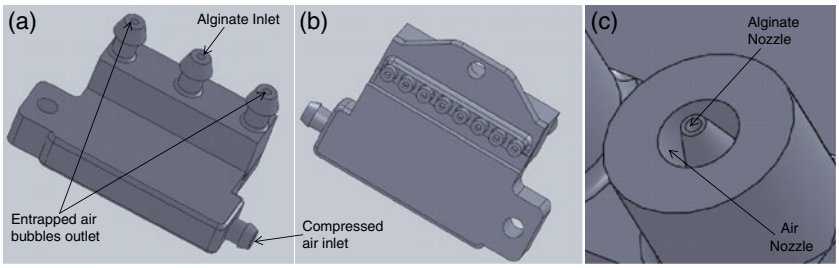

Fig. 1 (**a**) Isometric Top View (**b**) Isometric Bottom View and (**c**) close up view of the co-flow outlets in the microfluidic device

(Fig. 1(b)), each having 380 micrometers inner diameter which produce hydrogel microcapsules. These nozzles are concentrically surrounded by air nozzles with 2 mm inner diameter (Fig. 1(c)). There are two tubes connected at the top to allow the entrapped air bubbles to escape through them as the alginate solution fills up the chamber. Once all the entrapped air escapes through the two tubes the valves on the tubes are closed to prevent the alginate from rising in these tubes. In order to generate hydrogel microcapsules, alginate solution is introduced into the alginate chamber and compressed air is introduced in the air inlet. Figure 2 shows the alginate-cell mixture and compressed air flowing through the microfluidic device. The air enters the microfluidic device along the Z direction, then takes a 90° turn along the Y direction and then turns another 90° where it co-flows along with the alginate-cell mixture (inner nozzle) in the two concentric nozzles. The alginate-cells mixture enters the device along the X direction as shown to fill the inner chamber where it gets splits up into smaller streams and flows through the inner channels in the co-flow section, surrounded by air flow (outer nozzle). A variable flow pump 115 V (Thermo Fisher Scientific Inc., USA) is used to pump alginate solution into the microfluidic device. Tygon® tubing (Fisher Scientific, USA) is used to connect in-house air supply to the air channel and peristaltic/syringe pump to the alginate chamber. A pressure regulator is used to control the flow rate of air. The schematic diagram of the experimental setup is shown in Figs. 3 and 4. As the alginate solution is pumped into the microfluidic device it fills up the chamber and then starts flowing out through the internal alginate nozzle. The air flowing through the outer nozzle then shears off the alginate solution and form droplets which are collected in a calcium chloride bath where the hydrogel microcapsules crosslink to form microcapsules as shown in Fig. 3. These droplets thus formed are then further analyzed for shape, size, etc. under a high resolution microscope. The relative air/alginate flow ratios can be used to control the size of the droplets formed.

2.2 Design and fabrication

The microfluidic device was designed using SolidWorks 2008™ (Dassault Systemes Solidworks Corp., MA, USA) a commercially available CAD package. The CAD file is saved as a STL file which is the standard format for stereo lithography applications. After the CAD file is converted to STL file it is analyzed for defects and features that may not form. It is then prepared for high resolution build using 3D Lightyear software for the Viper si2 SLA System (3D Systems Corporation, South Carolina, USA). The parts were

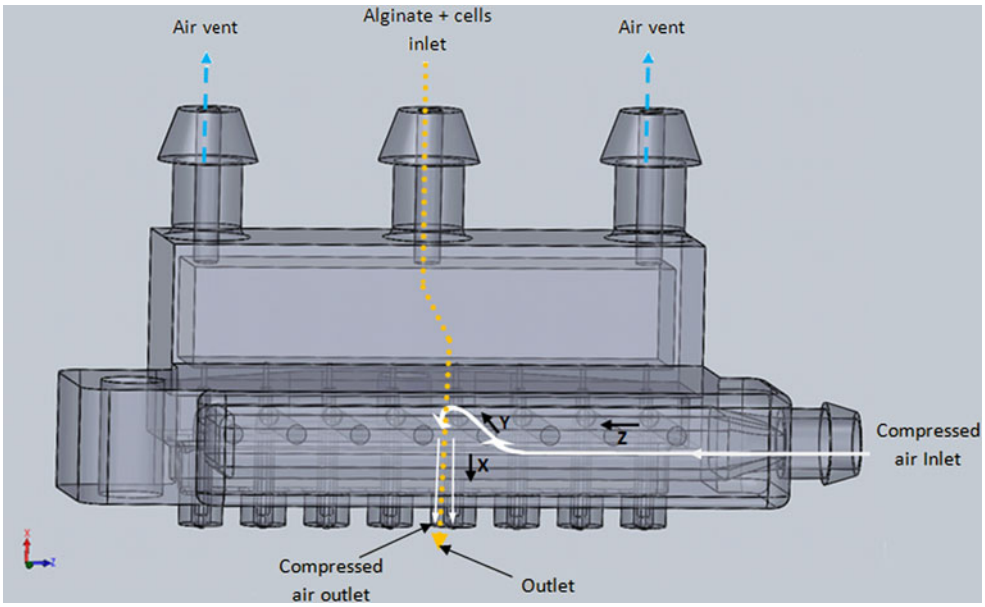

Fig. 2 Shows the flow of alginate-cell mixture and compressed air through the microfluidic device

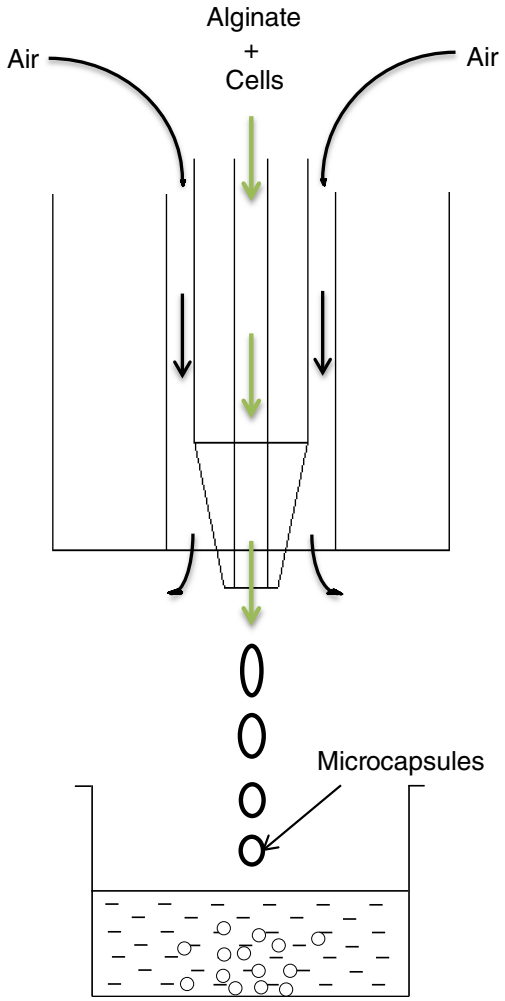

Fig. 3 2D Schematic of the droplet forming region of the microfluidic device

then built in the machine by UV curing of layers 0.002″ thick into a vat of liquid polymer. As the part is built in a vat of liquid resin appropriate supports are provided to support the structure. DSM Somos ProtoTherm 12120 polymer (3D Systems Corporation, South Carolina, USA) is the liquid resin used to build this device. After the build is complete, the excess liquid resin that is clinging to the parts is cleaned off by using a two step process. The first step comprises of cleaning using solvent called 'Polyflush' a type of propanol which removes bulk of the uncured resin. In the second step, isopropyl alcohol is used to remove Polyflush residue, which evaporates quickly and leaves the part clean and residue-free. After the part is cleaned it is then post cured in a UV oven for an hour. Following post cure, the supports break off easily from the part. After sanding, the parts can be sand blasted to provide a better surface finish.

2.3 Fluorescence labeling and protein encapsulation

Alexa 568-carboxy was coupled to bovine serum albumin (BSA) by taking 435 μl of 2.3 mg/ml of BSA in PBS in a 2 ml flip cap vial, and adding 28.8 μl of 1 mg/ml of EDAC (Sigma), 32.6 μl of 1 mg/ml of sulpho-NHS (Pierce), 3 μl of AlexaFlor568-carboxy-succinimide (in DMF). This mixture was allowed to react overnight at room temperature on stir plate and covered with aluminum foil. The above solution was dialyzed exhaustively with 4 buffer changes (1 L PBS buffer solution) using a 3.5 kDa dialysis tubing, 0.5–3 ml capacity. The Bio-Rad protein assay was used to determine the concentration of BSA after dialysis.

2.4 Isolation of islets from rat pancreas

Islets were isolated from the pancreas of Lewis rats (300–400 g) using the protocol of collagenase digestion of pancreatic tissue Lacy and Kostianovsky (1967) with modifications Field et al. (1996). Following euthanasia according to IACUC guidelines, the common bile duct was cannulated and 5 mL of 0.25 mg/mL Liberase TL (Roche, Indianapolis) in HEPES-buffered Hanks balanced salt solution (HBSS) was infused to distend the pancreas prior to incubation at 37°C for 15 min. The digestion was stopped with the

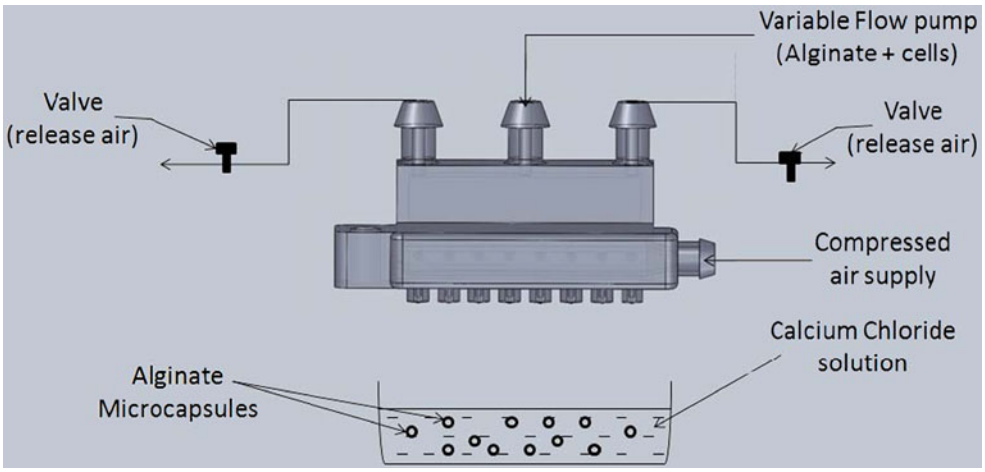

Fig. 4 Schematic of a complete encapsulation system using the microfluidic device

addition of 15 mL ice-cold wash solution (HEPES-buffered HBSS with 10% fetal bovine serum (FBS), and then shaken for 10 s to dissociate the digested pancreas. The digest was filtered through a 500 μm mesh filter and then washed three times with wash solution and centrifuged at 250*g* for 3 min. Islets were then handpicked under a stereomicroscope, or purified on a Histopaque gradient prior to handpicking, and cultured overnight at 37°C, 5% CO_2 in RPMI-1640 with 3.3 mM glucose and 10% FBS at a concentration of 15 islets per mL.

2.5 Microencapsulation of islets

Islets were microencapsulated as previously described Darrabie et al. (2005) using the 8-channel microfluidic device. Following purification, islets were suspended in 3% alginate solution (ultrapure low-viscosity high-mannuronic acid (LVM) sodium alginate, NovaMatrix, Oslo, Norway), and microspheres (<600 μm) containing one islet/microsphere were collected in 100 mM $CaCl_2$ bath where they were gelled during 15 min incubation. Following two washings with normal saline, the microspheres were incubated in 0.1% (w/v) Poly-L-Ornithine (PLO, Sigma-Aldrich, St. Louis, MO) for 10 min to provide them with perm-selectivity. In order to prevent electrostatic interactions between the positive charges on the polycationic PLO and the negative charges on cells and proteins in the body when the PLO-coated microcapsules are used for *in vivo* experiments, the PLO is covered by a final coating with the biocompatible poly-anionic alginate. Therefore, after two washings in normal saline, the PLO-coated microcapsules were incubated in 0.25% alginate solution for 4 min followed by two saline washes. The microcapsules were then incubated in 55 mM sodium citrate for 10 min to liquefy the inner alginate core prior to two final washes with normal saline. The liquefaction of the inner alginate core is performed in order to enhance the diffusion of nutrients, oxygen, and insulin, as previously shown by Garfinkel et al. (1998).

2.6 Histological tests of encapsulated islet viability

Following encapsulation, islets were fluorescently labeled for viability with carboxyfluorescein diacetate (CFDA) and propidium iodide (PI) to demonstrate live and necrotic cells respectively. Briefly, capsules were incubated with CFDA in serum-free RPMI 1640 for 15 min at 37°C, followed by washes in normal saline and a two-minute incubation with PI, prior to fixation with 4% paraformaldehyde and nuclear counterstaining with 4′, 6-diamidino-2-phenylindole (DAPI). *Student's t-test* was used to evaluate the significance of difference in percent viability of encapsulated versus unencapsulated islet cells, and a value of $p<0.05$ was accepted as significant.

3 Results

In this study, the effects of varying the flow rate of the aqueous phase, the shearing phase (by varying air pressure), alginate viscosity (by varying concentration), droplet formation time (through varying the distance between the nozzle tip and the gelation phase) were evaluated. Different droplet sizes and shapes were obtained by varying the flow rates of the aqueous phase (alginate) and the shearing phase (air), by changing the distance between the outlet nozzles and the collection plate and by varying the concentration of alginate by weight. Hydrogel microcapsules with diameters ranging from 400 μm to 1 mm can be produced with this microfluidic device. The formation of satellite particles was observed under various conditions. The satellite particles being smaller than the hydrogel microcapsules are lighter and can be easily separated from the desired microsphere samples. All the graphs are made by ignoring the satellite particles. The hydrogel microcapsules collected for each condition were allowed to crosslink for 15 min in the calcium chloride bath. After cross-linking, the microspheres were washed with water to remove excess calcium chloride and then stored in calcium-supplemented saline (saline + 0.25% $CaCl_2$) solution Moya et al. (2009). Small samples were randomly collected from the batch samples using transfer pipettes. Data for further study of geometry of the capsules was collected from smaller samples. Fifty diameter measurements were taken from each of these samples using Olympus BH-2 UMA (Olympus Corporation, USA). A high speed video camera (HotShot Mega Sc, NAC Image Technology, CA, USA) was used to capture the formation of microcapsules at 10000fps. The number of capsules formed by one nozzle over 500 ms was counted. . Results show that 18 capsules were formed per nozzle per sec at 82 ml/h using 1.5% Alginate solution. The factors affecting the formation of hydrogel microcapsules using the microfluidic device were assessed as follows:

3.1 Effect of flow rate of alginate

It was observed that the size of the hydrogel microcapsules decreases with reduction in the flow rate of alginate. Figure 5 is an illustration of the distribution of microcapsule size relative to alginate flow rate. As the flow rate of alginate is increased from 49.08 ml/h to 79.79 ml/h the average diameter of the microspheres increases from 654 μm to 707 μm.

3.2 Effect of change in air pressure

The size of the alginate hydrogel microcapsules is reduced with increase in the air pressure. Figure 6 illustrates the distribution of size with change in the air pressure from

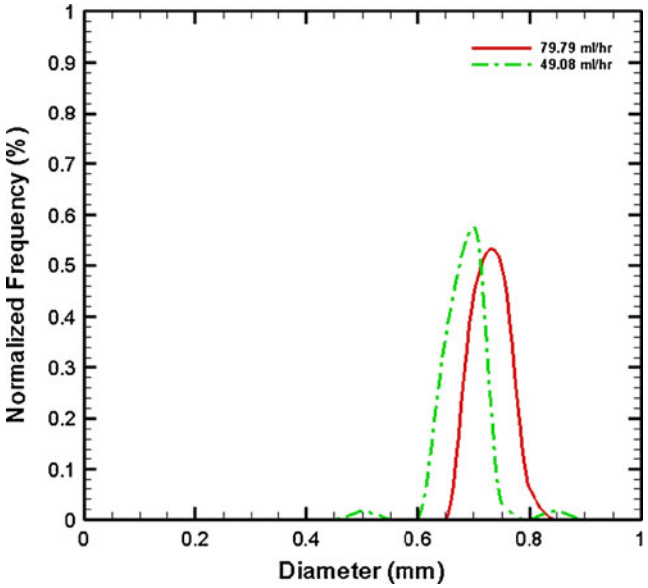

Fig. 5 Effect of flow rate of alginate on droplet diameter distribution

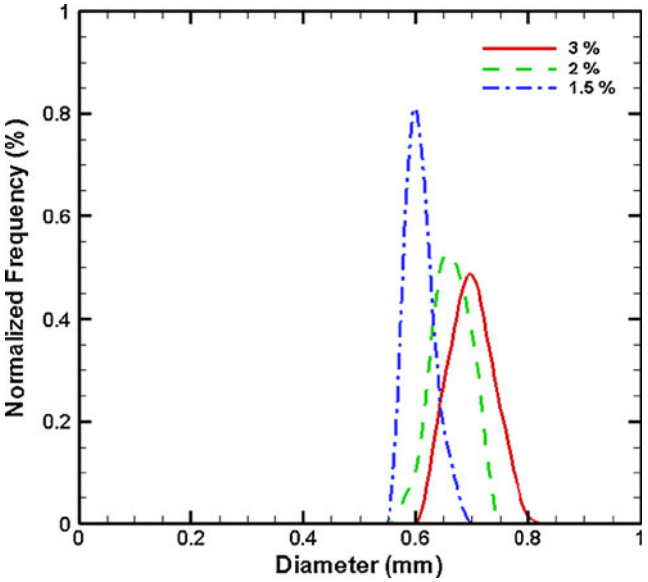

Fig. 7 Effect of concentration of alginate on droplet diameter distribution

5 psi to 2 psi and alginate flow rate of 42 ml/h. As the air pressure increased from 2 psi to 5 psi the average diameter of the hydrogel microcapsules decreased from 624 μm to 584 μm.

3.3 Effect of concentration of alginate

Figure 7 shows the effect of varying the alginate concentration at a fixed air pressure of 5 psi and alginate flow rate of 42 ml/h on size distribution. As the concentration of alginate is increased from 1.5% to 3%, the average diameter of the hydrogel microcapsules increased from 587 μm to 672 μm.

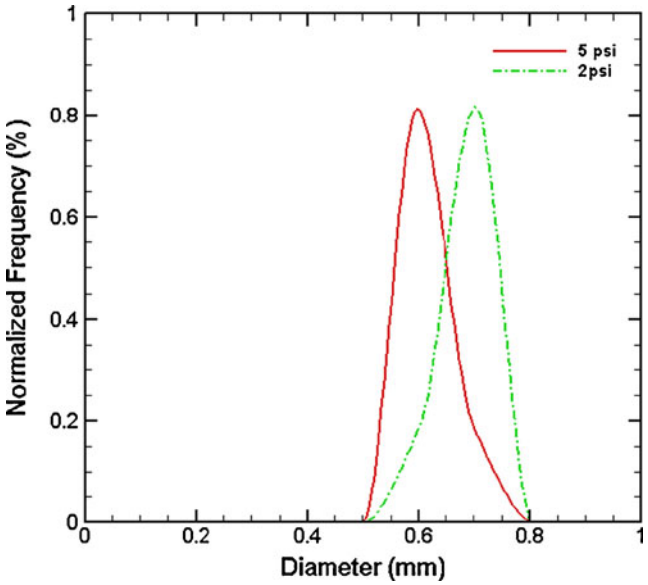

Fig. 6 Effect of air pressure on droplet diameter distribution

3.4 Effect of distance from collection plate

As the distance of the collection plate from the outlet nozzles is reduced below 0.24 m the shape of the microcapsules changes from circular to tear drop to random shapes. The optimum distance range observed was 0.24–0.29 m. As the distance increases beyond 0.29 m the shape of the microcapsules is spherical; however, it leads to the *coalescence* of the hydrogel microcapsules from adjacent nozzles as they fall into the collection plate. Figure 8(a), (b) and (c) show images taken with an optical microscope at 5x magnification.

3.5 Encapsulation of Bovine Serum Albumin (BSA)

BSA was encapsulated in capsules and to demonstrate the encapsulation of protein using the microfluidic device. Figure 9 shows fluorescence images of BSA encapsulated in alginate microcapsules. The bright red spots show the encapsulated protein. Figure 9(a) & (b) show images taken at 10x magnification.

3.6 Encapsulation of islet cells

For proof of concept, pancreatic islets isolated from normal Lewis rats were encapsulated using the high throughput microfluidic device. Under low magnification, pancreatic islets can be observed within the capsules as white spheroids approximately 100–200 μm in size, with one islet per capsule (Fig. 10(a), (b)). We also examined the effect of the encapsulation procedure on

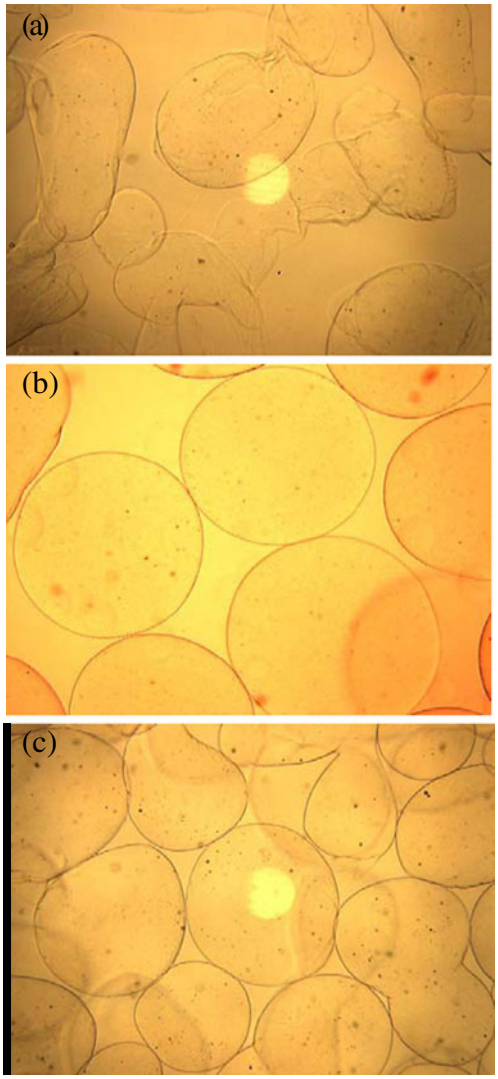

Fig. 8 Effect of distance of Calcium Chloride ($CaCl_2$) bath from tip of microfluidic device on droplet shape (**a**) 0.19 m—Irregular shapes (**b**) 0.25 m—Spherical droplets (**c**) 0.33 m—Irregular shapes

the viability of the pancreatic islets shown in Fig. 10(c) where live cells are green necrotic (dead) cells are red within the islet (Fig. 10(c)). We incubated unencapsulated islets and encapsulated islets in RPMI-1640 for 3 h, after which they were stained with the live-dead assay and the images quantitatively assessed for live and dead cells under a confocal microscope using Image J software (NIH) on the z-stack confocal images. Interestingly, statistical analysis of the percent viability of cells indicated that the% mean ± SD encapsulated islet viability (60.4±3.6) was significantly higher than that of the unencapsulated islets (40.3±1.8, p=0.001, n=3). These data are consistent with the observations by other investigators who have examined the effect of encapsulation on the viability of other cell types as discussed in the next section.

4 Discussion

Microencapsulation of islets prior to transplantation is designed to overcome the two major barriers to the use of islet transplants to treat Type 1 diabetic patients, which are inadequate availability of human islets and the need to use immunosuppressive drugs to prevent transplant rejection (Uludag et al. 2000; Opara and Kendall 2002; Lim and Sun 1980; Lanza and Chick 1997; Weir and Bonner-Weir 1997; Leblond et al. 1999). Since the introduction of this technique Lim and Sun (1980), numerous studies have been performed and have yielded variable results in large animal and human studies (Soon-Shiong et al. 1994; Sun et al. 1996; Dufrane et al. 2006; Calafiore et al. 2006; Wang et al. 2008; Thanos and Elliott 2009; Tuch et al. 2009), as many factors determine the outcome of encapsulated islet transplantation, including the length of time required to encapsulate enough islets for such studies. The length of time required to encapsulate sufficient quantities of islets for transplantation is a critical factor that affects the outcome of their transplantation, because a prolonged process of encapsulation results in decreased viability of the islets Opara et al. (2010). Invariably, good product quality control is very difficult to achieve with the very slow microencapsulation devices currently available for encapsulating islets for transplantation. There is therefore a desperate need for throughput microencapsulation devices to provide better product

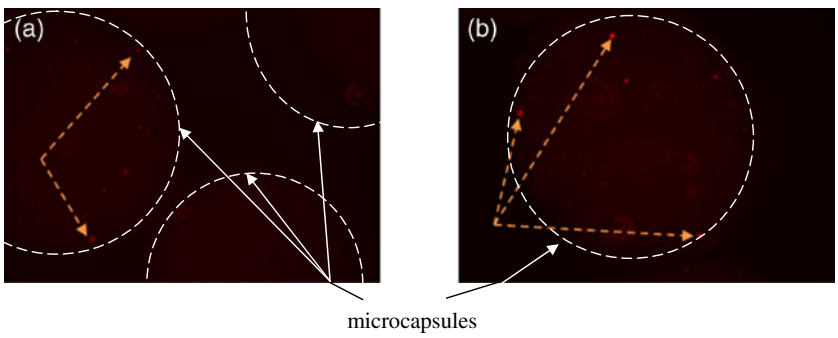

Fig. 9 (**a**) & (**b**): Protein (BSA) encapsulated hydrogel microcapsules. *Arrows* indicate the location of protein in the image

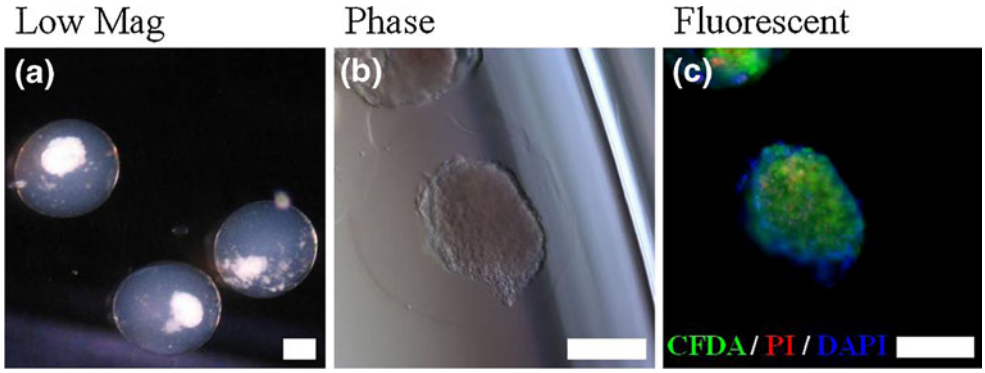

Fig. 10 Encapsulation of rat pancreatic islets with microfluidic device. (**a**) Islets seen within the alginate capsules; (**b**) parallel phase contrast and (**c**) fluorescently labeled pancreatic islets for live and dead cells, stained with carboxyfluorescein diacetate (CFDA; *green*) and propidium iodide (PI; *red*) respectively, and nuclear counterstain 4′, 6-diamidino-2-phenylindole (DAPI; *blue*). Scale bars=200 μm

quality control if encapsulated islet transplantation is going to become a clinically viable procedure. The microfluidic approach in microencapsulation described in this paper is capable of producing large numbers of alginate microspheres to encapsulate cells and proteins. Due to scalability of our monolithic microfluidic device without increasing complexity, we have demonstrated 8x production rates by scaling our device with 8 outlets as compared to a single co-flow device. It can be scaled to 64 outlets for instance and produce at a rate of 64x. The new prototype device that we have designed is capable of increasing by 8 times the rate of production of microspheres compared to currently available devices, and can be scaled up even higher by a magnitude of 64 times. Consequently, the new microencapsulation approach could potentially reduce the previously mentioned 100 h required for the production of 1 million microencapsulated islets for human transplantation (de Vos et al. 1997) by several orders of magnitude- Indeed, millions of cells for many patients can be encapsulated in that same short duration, and the entire encapsulation process would be completed within this shorter time frame. In addition to producing large quantities of encapsulated cells in a very short period of time, one of the biggest advantages of this new procedure is that a given preparation of encapsulated cells will be subjected to the subsequent manual steps of perm-selective coating and washings at the same time, and this will have tremendous positive impact on the viability of the encapsulated cells resulting in good product quality control. In addition, the use of air rather than oil/water emulsions to generate droplets in our encapsulation procedure with the prototype device obviates the need to remove the oil phase thus reducing the duration of the microencapsulation process.

Our data showing a much higher viability of encapsulated islets compared to unencapsulated islets is consistent with observations by other investigators (Chin et al. 2008). We believe that encapsulating islets may actually enhance their function *in vitro* culture compared to un-encapsulated naked islets because the 3-D support provided by the microspheres results in a better microenvironment for the delivery of oxygen and nutrients to encapsulated cells. It has previously been shown that the 3D structure of alginate microspheres used to encapsulate HepG2 liver cells enhanced the metabolic activity of the cells compared to un-encapsulated cells in the studies performed by Chin and colleagues.

It has been previously shown that alginate microspheres can be used to encapsulate therapeutic proteins for controlled drug delivery (Gombotz and Wee 1998; Moya et al. 2009; Moya et al. 2010), and in this paper, we have shown that the microfluidic device can also be used to encapsulate proteins, thus making it useful for pharmaceutical scale manufacture of microcapsules for controlled drug delivery.

One potential pitfall of the microfluidic approach to microencapsulation is the generation of satellite microparticles measuring approximately 10–20 μm in diameter, which occurs without adequate adjustments in the alginate flow rate and air pressure. However, when these factors are optimally controlled, the formation of these satellite microparticles has been either completely eliminated or kept to the barest minimum during microencapsulations with the prototype device. Another issue that we are still working on as we further develop the device is that using our optimal ratio of cell/alginate ratio of 5,000 islets/ml, the ratio of empty to cell-containing droplets is presently more than 20%, and we are currently trying to incorporate into the process a technique to separate the empty capsules from the cell-containing capsules based on their density difference.

In summary, we have designed a scalable microfluidic prototype device suitable for encapsulating therapeutic proteins for controlled drug delivery and for microencapsulating cells for transplantation in the treatment of a variety of diseases, particularly islets for transplantation in diabetic patients. This microfluidic approach to microencapsulation is an effective throughput device for generating microspheres for clinical cell therapy and controlled drug delivery at a large scale.

Acknowledgements The authors acknowledge the financial support of the National Institutes of Health (GRANT # RO1DK080897), the Rosenfeld Estate, Greenville, NC for research in Dr. Opara's laboratory and the National Science Foundation IR/D Program for providing travel support for Dr. M. K. Ramasubramanian to direct the research at North Carolina State University. Any opinion, findings, and conclusions or recommendations expressed in this material are those of the authors and not necessarily reflect the views of the funding organizations.

References

D.J. Beebe, G.A. Mensing and G.M. Walker, Annu. Rev. Biomed. Eng. (2002) doi:10.1146/annurev.bioeng.4.112601.125916

R. Calafiore, G. Calabrese, G. Basta, G. Luca, A. Lemmi, M. Montanucci, L. Racanicchi, F. Mancuso, P. Brunetti, Diabetes Care **29**, 137–138 (2006)

M. Chabert, J.-L. Viovy, Proc. Natl. Acad. Sci. U. S. A. **105**(9), 3191–3196 (2008)

K. Chin, S.F. Khattak, S.R. Bhatia, S.C. Roberts, Biotechnol. Prog. **24**, 358–366 (2008)

M.D. Darrabie, W.F. Kendall, E.C. Opara, Biomaterials **26**(34), 6846–6852 (2005)

J. de Jong, R.G.H. Lammertink and M. Wessling, Lab Chip (2006) doi:10.1039/b603275c

P. De Vos, B.J. De Haan, R. Van Schilfgaarde, Biomaterials **18**, 1085–1090 (1997)

D.C. Duffy, J.C. McDonald, O.J.A. Schueller, G.M. Whitesides, Anal. Chem. **70**, 4974–4984 (1998)

D. Dufrane, R.M. Goebbels, A. Saliez, Y. Guiot, P. Gianello, Transplantation **81**(9), 1345–1353 (2006)

J. Field, A. Farney, D. Sutherland, Transplantation **61**(10), 1554–1556 (1996)

M.R. Garfinkel, R.C. Harland, E.C. Opara, J. Surg. Res. **76**, 7–10 (1998)

W.R. Gombotz, S.F. Wee, Adv. Drug Deliv. Rev. **31**, 267–285 (1998)

V. Haverkamp, W. Ehrfeld, K. Gebauer, V. Hessel, H. Lowe, T. Richter, C. Wille, Fresenius' J. Anal. Chem. **364**, 617–624 (1999)

B.R. Hsu, H.C. Chen, S.H. Fu, Y.Y. Huang, H.S. Huang, J. Formos. Med. Assoc. **93**, 240–245 (1994)

A. Joly, J.F. Desjardins, B. Fredmond, M. Desille, J.P. Campion, Y. Malledant, Y. Lebreton, G. Semana, F. Edwards-Levy, M.C. Levy, B. Clement, Transplantation **63**, 795–803 (1997)

I. Kobayashi, S. Mukataka, M. Nakajima, Ind. Eng. Chem. Res. **44**, 5852–5856 (2005)

P.E. Lacy, M. Kostianovsky, Diabetes **16**, 35–39 (1967)

R.P. Lanza, W.L. Chick, Surgery **121**, 1–9 (1997)

F.A. Leblond, G. Simard, N. Henley, B. Rocheleau, P.M. Huet, J.P. Hallé, Cell Transplant. **8**, 327–337 (1999)

R.H. Li, Adv. Drug Deliv. Rev. **33**(1–2), 87–109 (1998)

F. Lim, A.M. Sun, Science **210**, 908–910 (1980)

K. Mae, T. Maki, I. Hasegawa, U. Eto, Y. Mizutani, N. Honda, Chem. Eng. J. (Amsterdam, Neth.) **101**, 31–38 (2004)

M.L. Moya, S. Lucas, M. Francis-Sedlak, X. Liu, M.R. Garfinkel, E.C. Opara, E.M. Brey, Microvasc. Res. **78**, 142–147 (2009)

M.L. Moya, J.J. Huang, M.E. Francis-Sedlak, S.W. Kao, E.C. Opara, M.H. Cheng, E.M. Brey, Biomaterials **31**, 2816–2826 (2010)

J. Narasimhan, I. Papautsky, J. Micromech. Microeng. **14**, 96–103 (2004)

T. Nisisako, T. Torii, Lab Chip **8**, 287–293 (2008)

E.C. Opara, W.F. Kendall, Expert. Opin. Biol. Ther. **2**, 503–511 (2002)

E.C. Opara, S.H. Mirmalek-Sani, O. Khanna, M.L. Moya, E.M. Brey, J. Investig. Med. **58**(7), 831–837 (2010)

G. Orive, R.M. Hernandez, A.G. Rodriquez, R. Calafiore, T.M. Chang, P. de Vos, G. Hortelano, D. Hunkeler, I. Lacik, J. Pedraz, Trends Biotechnol. **22**(2), 87–92 (2004)

P. Soon-Shiong, R.E. Heintz, N. Merideth, Q.X. Yao, Z. Yao, T. Zheng, M. Murphy, M.K. Moloney, M. Schmehl, M. Harris, R. Mendez, R. Mendez, P.A. Sandford, Lancet **343**, 950–951 (1994)

J. Steigert, S. Haeberle, T. Brenner, C. Muller, C.P. Steinert, P. Koltay, N. Gottschlich, H. Reinecke, J. Ruhe, R. Zengerle, J. Ducree, J. Micromech. Microeng. **17**, 333–341 (2007)

S. Suguira, T. Oda, Y. Aoyagi, R. Matsuo, T. Enomoto, K. Matsumoto, T. Nakamura, M. Satake, A. Ochiai, N. Ohkohchi, M. Nakajima, Biomed. Microdevices **9**, 91–99 (2007)

Y. Sun, X. Ma, D. Zhou, I. Vacek, A.M. Sun, J. Clin. Invest. **98**, 1417–1422 (1996)

C.G. Thanos, R.B. Elliott, Expert. Opin. Biol. Ther. **9**(1), 29–44 (2009)

B.E. Tuch, G.W. Keogh, L.J. Williams, W. Wu, J.L. Foster, V. Vaithilingam, R. Philips, Diabetes Care **32**, 1887–1889 (2009)

H. Uludag, P. De Vos, P.A. Tresco, Adv. Drug Deliv. Rev. **42**, 29–64 (2000)

T. Wang, J. Adcock, W. Kuhtreiber, D. Qiang, K.J. Salleng, I. Trenary, P. Williams, Transplantation **85**, 331–337 (2008)

G.C. Weir, S. Bonner-Weir, Diabetes **46**, 1247–1256 (1997)

G.M. Whitesides, Nature (2006) doi:10.1038/nature05058

G.H.J. Wolters, W.M. Fritschy, D. Gerrits, R. Van Schilfgaarde, J. Appl. Biomater. **3**, 281–286 (1992)